Pergamon

PII: S0306-4522(97)00213-3

Neuroscience Vol. 82, No. 1, pp. 69–81, 1998

0306–4522/98 $19.00+0.00

STEP CYCLE-RELATED OSCILLATORY PROPERTIES OF INFERIOR OLIVARY NEURONS RECORDED IN ENSEMBLES

S. S. SMITH

Department of Neurobiology and Anatomy, MCP-Hahnemann School of Medicine, Allegheny University of the Health Sciences/EPPI, 3200 Henry Avenue, Philadelphia, PA 19129, U.S.A.

Abstract—This study was conducted to characterize patterns of discharge from the dorsal accessory olive during different behavioural states. To accomplish this goal, adult rats were chronically implanted with arrays of microwires (25–50 μm) to record from as many as 23 neurons from the dorsal accessory olive bilaterally during locomotor paradigms or at rest. Olivary neurons discharged sporadically at low firing frequencies (1–5 Hz) when the rat was at rest. However, during locomotor paradigms involving constant speed treadmill locomotion, olivary neurons discharged rhythmically at frequencies which closely matched step cycle frequencies. The rhythmic nature of olivary discharge was maintained even during brief periods of inconsistent gait. During treadmill locomotion utilizing variable acceleration/deceleration paradigms olivary neurons discharged at 3 Hz frequencies. Electrical stimulation of peripheral afferents resulted in rhythmic discharge of olivary neurons at frequencies harmonic with the rate of stimulation.

These data suggest that oscillatory patterns of discharge exhibited by the inferior olivary nucleus are only seen during rhythmic behavioral tasks or stimulation paradigms. Further, the dissociation between the rhythmic nature of the task and the continued oscillation suggests that oscillatory activity of the inferior olive may be due both to an intrinsic rhythm as well as related to ongoing sensorimotor input.

Key words: step cycle, locomotion, inferior olive, oscillation, neuronal ensemble, synchronization.

The inferior olivary (IO) complex has been reported to act as an internal timing device for coordinated movement.[12] Axons from the dorsal accessory olive (DAO) project to sagittally aligned rostrocaudal rows of Purkinje cells within the paravermal cerebellum, where they transmit rhythmic signals[12] to the cerebellar cortex. The IO is a particularly good candidate for a timing device because this structure has been shown to exhibit subthreshold oscillations of membrane potential[4,11,13,16,32] with frequencies in the range of 3 to 10 Hz. This frequency range parallels that reported for rapid movements of the limbs and digits.[12] Intracellular recording in the brainstem slice preparation[11,16,17,32] has revealed that an action potential generated in an olivary neuron is characterized by a Na^+ and Ca^{2+}-dependent depolarization, followed by a K^+-dependent hyperpolarization. Hyperpolarization of the membrane deinactivates a low-threshold Ca^{2+}-dependent rebound spike which triggers the oscillation. Rhythmic membrane oscillations are also dependent upon the presence of dendrodendritic gap junctions[9,20,26] as coupling between neurons has been shown to be essential in maintaining rhythmic discharge of an olivary population.[12]

Abbreviations: DAO, dorsal accessory olive; IO, inferior olive.

In vivo studies have demonstrated that climbing fibre activity of the cerebellum, the all-or-none output from the IO, is rhythmic following brief stimulation of the upper lip or forepaw.[6,11,14,21,30] Rhythmic behaviours such as licking have also been shown to be associated with rhythmic climbing fibre activity.[30] Some studies have also noted rhythmic climbing fibre activity associated with the step cycle,[10] although other reports have failed to replicate this finding.[1] Unlike Purkinje cell simple spike discharge which is normally associated with the stance phase of locomotion,[1,23] climbing fibre responses have been noted during transitions of the step cycle;[10] i.e. changes from swing to stance or stance to swing.

The purpose of the following study was to investigate rhythmic olivary activity during the step cycle using chronically implanted microwire bundles in rats trained to locomote on a moving treadmill. One goal was to characterize the receptive field properties of rhythmically firing DAO neurons. As there is no clear consensus in the literature as to the correlation between olivary discharge and the step cycle, this study also sought to examine this relationship using neuronal ensemble recording techniques. This paradigm more easily permits identification of rhythmic discharge than does single electrode recording, as olivary oscillations have been shown to be an emergent property of a coupled olivary network,[12] and do

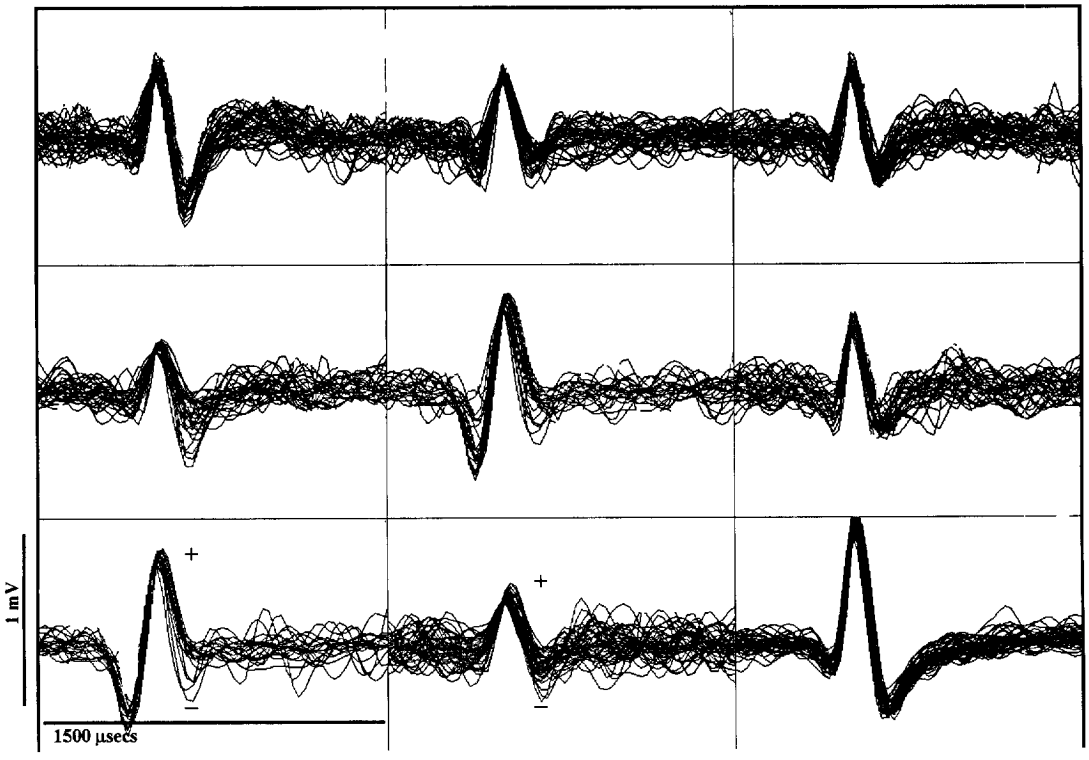

Fig. 1. Waveforms of nine olivary neurons recorded from six 50 μm microwires. Amplitude and polarity of the spikes are indicated.

not appear to be a property of individual neurons. An additional goal was to examine the relationship between intrinsic olivary rhythmicity and rhythmicity entrained by afferent inputs during limb stepping, as has been demonstrated for tongue movements.[30]

EXPERIMENTAL PROCEDURES

Animals

Adult, estrous female Long–Evans rats (200–250 g, Charles River) were used for all protocols. Animals were housed individually in a temperature-controlled facility under a constant light:dark cycle (14 h light:10 h dark). Food and water were available continuously. All efforts were made to minimize animal suffering, to reduce the number of animals used, and to utilize alternatives to *in vivo* techniques, according to IACUC regulations (Animal Welfare Assurance No. A-3191-01).

Surgical implantation

Rats were surgically implanted with Microtek headplugs consisting of two microwire bundles, each containing 5–8 stainless steel, teflon-coated 25–50 μm microwire electrodes (NB Labs, Denison, TX) as previously described.[19,23–25] The bundles were independently driven into forelimb or hindlimb projection areas of the dorsal accessory olive,[2] bilaterally (DAO, 11.5–12.8 mm caudal to bregma, 0.45–1.0 mm lateral, 7.0–8.75 mm from the pial surface). Correct placement of the electrodes was ensured by recording extracellular unit activity continuously from the microwires during the implantation.[3,8] Identification of characteristic neuronal firing properties was used to verify correct implantation within the DAO.[3,8] In addition, antidromic stimulation from the paravermal cerebellum was used to verify electrode placement within the DAO, as previously demonstrated.[25] Roughly 30–40% of the olivary spikes were inverted, with a negative potential. At the termination of all experimental protocols for one animal, lesions at recording wire sites were produced by direct passage of anodal current (100 μA, 10 s). Following preparation of brain tissue, brains were sectioned at 50 μm, stained with Cresyl Violet, and recording sites verified using light microscopy.

Neuronal ensemble recording

Simultaneous spiking activity of up to 32 single neurons was recorded through the individual microwires via i) a headstage containing field effect transistors to amplify current, which mimimizes artifact due to head movement, ii) a flexible wire harness and commutator, iii) a multichannel pre-amplifier box, and iv) a 64 channel amplifier-filter-discrimination recording system (Spectrum Scientific, Dallas TX) as previously described.[19,24,25] The waveforms of individual discriminated neurons were simultaneously visualized and stored on a 486 personal computer graphics screen (Fig. 1). Meanwhile their discharge times were recorded and stored on disk using a Motorola VME computer system using acquisition software written by J. Chapin and T. Bunn.

Discrimination technique

Routinely, up to two spikes, and rarely three, can be discriminated from each individual recording microwire. (See Fig. 1 for sample waveforms from nine leads recorded during this paradigm.) The on-line discriminators utilize Motorola 56000 digital signal processors which implement time and voltage windows for spike detection. For further verification that single neuron action potentials are being detected, a principal components analysis-based waveform

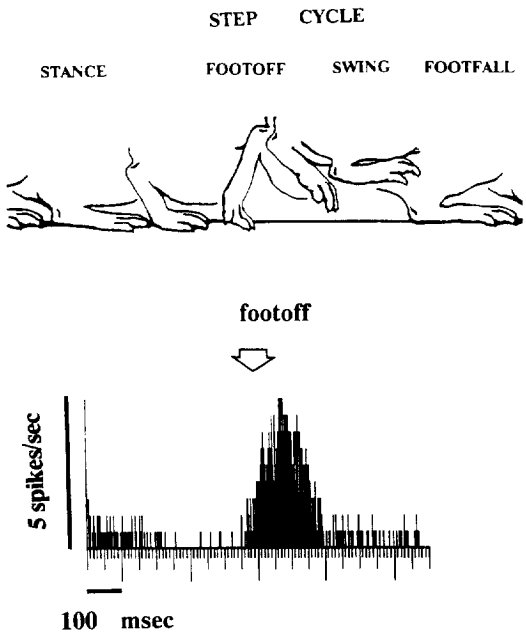

Fig. 2. Discharge from the DAO is correlated with the step cycle. Olivary neurons with receptive fields on the upper hindlimb discharged in bursts during the transition from swing to stance, as demonstrated by the peri-event histogram constructed around the onset of the swing phase (foot-off). This correlation was not observed from cells with receptive fields on the distal limbs. (Data are representative of 74 cells recorded from five rats.)

recognition scheme is used.[7] The algorithms transform 32 points of each waveform to a two-dimensional system that can be plotted graphically and visualized to i) verify spike isolation and ii) maintain recordings from the same neurons over a period of days. Roughly 60–80% of the recorded neurons could be discriminated as a single spike, the remainder being multiple neurons (1+), a phenomenon which is well-suited to the determination of synchronized olivary oscillations which are known to be emergent properties of neuronal ensembles, rather than individual spikes.[12] Over a three week recording period, over 70% of the neurons remain stable based on this criteria.[23–25] The 50 μm microwires are now well established for successful recordings of individual neurons from numerous CNS sites.[19,24,25] Although in some cases, DAO (single- or multiple-units) attained high levels of discharge (5 spikes/s), high rates of activity such as these have been reported previously by other laboratories,[3] especially in response to electrical or behavioural stimuli. DAO discharge was correlated with the step cycle (stance-to-swing) during treadmill locomotion (Fig. 2).

Behavioural paradigms

Treadmill locomotion. Rats were run on a treadmill at a constant speed (4 or 11 cm/sec) or at random speeds produced by sudden accelerations or decelerations (from $-12\ cm/s^2$ to $+12\ cm/s^2$), as previously described[24] (see Fig. 3). Over the 15 min period of random speed treadmill locomotion, the treadmill was on for 10 s periods alternating with 10 s off periods. For the resulting 450 s of treadmill movement, the treadmill speed was changed every 0.25 s and acceleration/deceleration changes (direction) accomplished every 0.5 s; the total time spent at each acceleration/deceleration rate totalled approximately 9 s (increments of $0.25\ cm/s^2$) over the -12 to $+12\ cm/s^2$ range. Although the duration of each treadmill speed change was consistent, the sequence of speed changes and the direction of those changes were randomly generated.

Inconsistent gait. Inconsistent gait obtained during constant speed treadmill locomotion was identified by periods of arrhythmic stepping as assessed by video analysis and autocorrelations of the step cycle. (In general, rhythmic gait was closely correlated with constant speed treadmill locomotion. Typically, inconsistent gait was only observed over 3–4 s periods intermittently throughout the paradigm.) This is in contrast to gait obtained during the variable acceleration paradigm, which, despite random changes in speed, was relatively rhythmic and consistent at faster frequencies (3 Hz). Changes in treadmill speed were compensated for by alterations in stride length rather than altered step cycle frequency.

Missed steps. A "missed" step is defined here as a step which is out of synchronization with the ambient step cycle rhythm (see Fig. 8); in all cases observed it was preceded by two steps in quick succession. Therefore it did not interfere with the overall gait of the animal, or cause the animal to stumble.

Analysis

Recordings from the IO during both paradigms were analysed using autocorrelation and cross-correlation procedures to determine: i) the number of neurons with synchronized activity, ii) the number of neurons with rhythmic activity, iii) the frequency of these oscillations, compared with the step cycle frequency, and iv) the receptive field properties of the recorded neurons. These parameters were determined as follows:

Synchronization. Synchronization was determined with a cross-correlation matrix ("Stranger" software) which averages firing of every neuron recorded with every other neuron (See Fig. 4). Note in this matrix all neurons are synchronized, except that neurons no. 1 and 4 are not synchronized with neurons 6–10 (noted by "ns" for non-significant). Here neuron no. 5 was designated as "driver" because it synchronized with the greatest number of neurons, with the greatest average r. Correlated discharge is determined by a peak distinguishable from background discharge ($P<0.01$) as determined by the one-dimensional Kolmogorov–Smirnoff method and graphically depicted in the data analysis program. In addition, a peak at the node (0 time point) reflects absolute coincident firing of the two neurons. From these correlograms (which employ a 20 ms time window and correlograms generated using 1 ms bins), the correlation coefficient can be calculated from the graph as: r(maximum discharge − mean discharge)/(1000 − bin size in ms). This is depicted in Fig. 4. Typically, at least 10^5 spikes were recorded from all neurons, over periods of 15–30 min. With this large number of spikes (n=100,000–200,000), the threshold for significance is $r \sim 0.01$. Statistical significance of the correlation coefficient was determined with the formula:[31]

$$r = tS_r$$

where t = Student's t, and

$$S_r = \sqrt{\frac{1 - r^2}{(n - 2)}}$$

where n is the number of data samples.

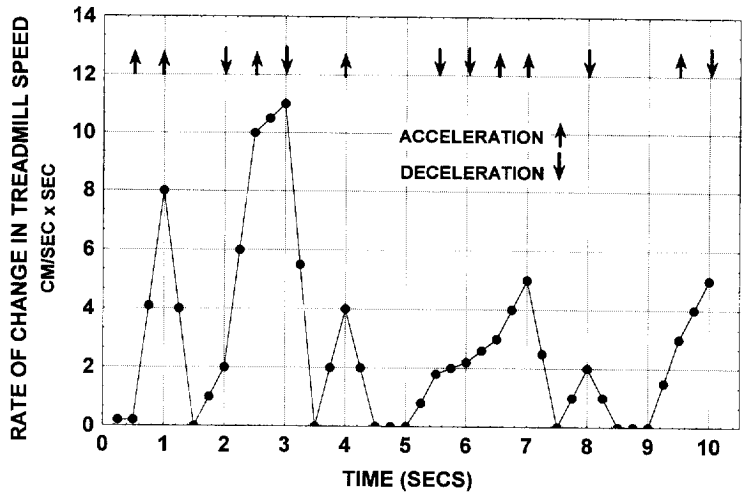

Fig. 3. The variable acceleration paradigm. A representative 10 s excerpt from the variable acceleration paradigm depicting typical random changes in speed. (Arrows indicate increases (up arrow) or decreases (down arrow) in speed).

As n was typically very large in this study (10^3–10^5), the above formula can be simplified as:

$$S_r = \sqrt{1/n}$$

Average r of a population was then calculated as: sum(r)/n for all significant cross-correlations of the matrix. Synchronization could be due to coupling or a common input peak; evidence for the former is demonstrated by a sharp (1 ms) peak at the node (± 1–2 ms), as was noted in the present study; a broader peak with greater time lag may suggest a common input peak.

Oscillations. An oscillation was defined as a deflection in firing rate greater than 20% of the maximal activity with a bilateral pattern of distribution as assessed using correlogram analysis.

Correlograms. Both auto- and cross-correlations of DAO discharge were used to determine the rhythmicity and synchronicity of olivary discharge. For this procedure, the activity of one "driver" neuron (chosen as the optimal driver) is used to create the nodes for cross-correlations between adjacent neurons[22] (see Fig. 4). Peri-event histograms were also obtained by averaging neuronal activity around particular phases of the step cycles of different limbs obtained using videoanalysis. The video system used is a Lafayette (Super VHS) with 16.67 ms resolution, and includes a motion analysis system. This allowed an accurate determination of the optimal motor correlate of each neuron. In addition, correlograms of the step cycle were constructed around the times of footfall, as determined by video analysis.

Stimulation protocols

Responses of DAO neurons to stimulation of the forelimb or hindlimb were tested using 8 mil teflon-coated, seven-stranded stainless steel wires (Medwire) with 1 mm exposed tips implanted subcutaneously in the forelimb area. The wires were threaded subcutaneously from the limb to the headplug. Computer controlled stimulations were delivered through a WPI biphasic constant current stimulator. Stimulus trains consisted of 2–3 monophasic rectangluar pulses (0.3–1.2 MA, 0.2 s each, 500 Hz every 2 s). Responses to stimulation were evaluated using using peri-event histograms and stripchart records.

RESULTS

Olivary discharge and constant speed locomotion

Olivary discharge recorded from five neuronal clusters (15–23 neurons/200 μm diameter/rat) exhibited synchronized rhythmic discharge during treadmill locomotion paradigms. An average of 65% of the neurons recorded from each population exhibited upper hindlimb receptive field properties; the remainder of the population exhibited upper forelimb properties. Peri-event histograms revealed that these neurons discharged maximally during transition from swing to stance during the step cycle (Fig. 2). In contrast, discharge recorded from cells with receptive fields on the distal limbs was not correlated with the step cycle (data not shown), but instead responded to event change (i.e. change in treadmill speed) as reported in earlier manuscripts.[8,24,25] The discharge recorded from the former subpopulation (upper limb sensory correlate) was tested for rhythmicity and synchronicity using auto- and cross-correlation techniques (see Fig. 4, for example of this technique to analyse data during the variable acceleration paradigm). Firing patterns tested during two different treadmill paradigms revealed rhythmic discharge of 0.7 and 1.3–1.5 Hz frequencies during treadmill locomotion at 4 and 11 cm/s, respectively (Fig. 5B,C). In contrast, rhythmic discharge was not observed during non-locomotor rest periods (Fig. 5A). Eighty per cent of the neurons exhibiting these oscillating patterns of discharge were synchronized (with phase lags from 0 to 2 ms), with an average correlation coefficient of 0.2 ($P<0.05$). The frequency range of the oscillation varied from 2–4 Hz (peak-to-trough).

Correlation of olivary rhythmicity with the step cycle

The correlograms of olivary discharge described above resembled step cycle-correlated discharge, as

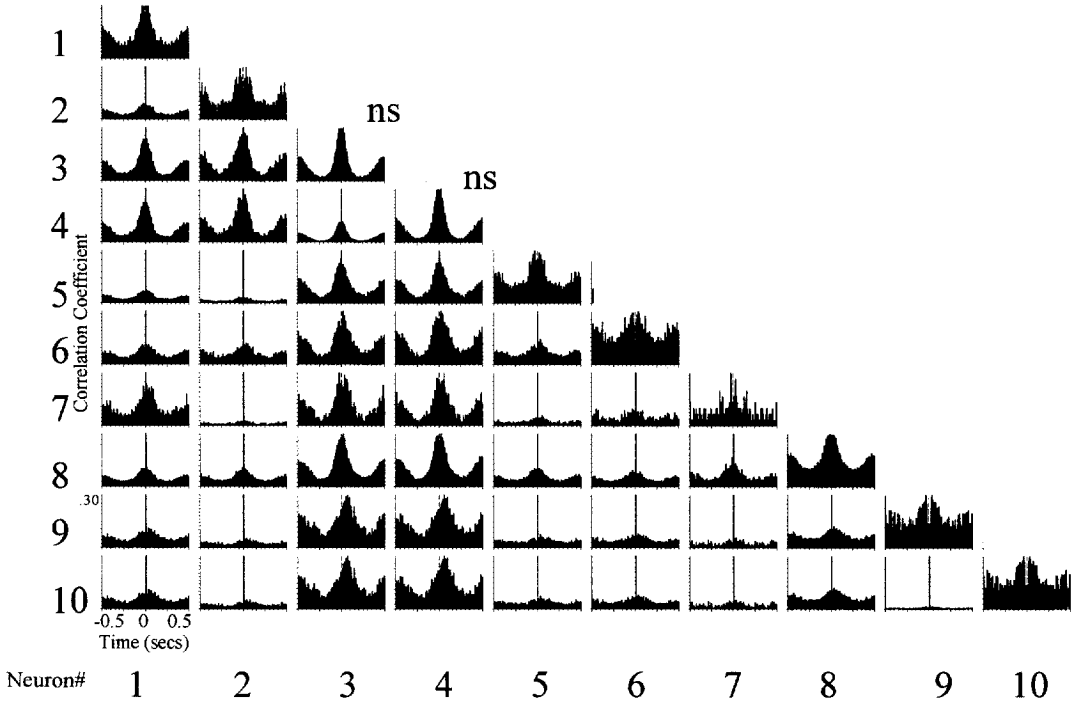

Fig. 4. Cross-correlation matrix analysis of neuronal coupling during the variable acceleration treadmill paradigm. A cross-correlation matrix (10 × 10 neurons) cross-correlates discharge from every recorded neuron with every other recorded neuron (indicated by nos 1–10). (Time base–*x*-axis; correlation coefficient, r–*y*-axis, r=0.3 for cell no. 8 is average for all neurons; all correlations are significant ($P<0.01$) except where noted ("ns", not significant). (See Experimental Procedures for algorithm used to calculate the correlation coefficient). Discharge from pairs of neurons (top and left) is correlated at the node (time of 0). Autocorrelograms (1 vs 1, etc.) emerge on the diagonal; in this case, the software eliminates the peak which must=1.0. For the remainder of the correlograms, a well-defined sharp peak above spontaneous discharge is indicative of coupling. Note that all neurons, except nos 1 and 4, are correlated with all other neurons. Neuron no. 5 is the "driver" in this case, because it exhibits the greatest r, and thus coupling, with the other neurons in the cluster. These data are representative of 75 cells recorded from three rats.

demonstrated by the peri-event histograms of olivary discharge averaged around foot-fall, presented in Fig. 6. In this case, the frequency of olivary "bursts" averaged around step cycle time points (swing-to-stance) was identical to that obtained using auto-correlation techniques, both in frequency and distribution (0.7 Hz; compare with Fig. 5).

In order to further compare the relationship between the step cycle and correlated discharge, autocorrelograms of step cycle time-points (Fig. 7C) during constant speed treadmill locomotion (4 cm/s) were compared with auto-correlograms of olivary discharge (Fig. 7A). Auto-correlations of the step cycle averaged around the onset of the stance phase during consistent locomotion resembled the correlograms of olivary discharge both in frequency and depth of modulation (i.e. also 0.7 Hz), suggesting that rhythmic olivary discharge is tightly coupled to step cycle rhythmicity.

Olivary rhythmicity during inconsistent gait

Correlograms of olivary activity constructed during periods of inconsistent gait revealed rhythmic patterns of olivary activity at harmonic frequencies (Fig. 7B) despite inconsistent and irregular patterns of gait, as assessed by autocorrelations of the step cycle constructed around foot-fall during inconsistent locomotion (Fig. 7D). These results are representative of those observed from 50 neurons recorded from five rats.

Olivary discharge and treadmill locomotion using a variable acceleration paradigm

During treadmill locomotion using a variable acceleration paradigm, step cycle frequency was proportional to treadmill speed. Thus, when assessed over a 10 s interval of varying treadmill speed, gait was non-rhythmic. However, when correlograms of the step cycle were constructed around foot-fall over a 1 s interval, a 3 Hz rhythm was revealed which indicates the minimum inter-step interval. Olivary discharge recorded during this paradigm exhibited rhythmic discharge of a similar 3 Hz frequency, as illustrated by the correlogram presented in Fig. 5D. Peak firing rate was higher than observed during periods of constant speed locomotion. On the average, 80% of the neurons recorded using this paradigm exhibited synchronized oscillatory patterns

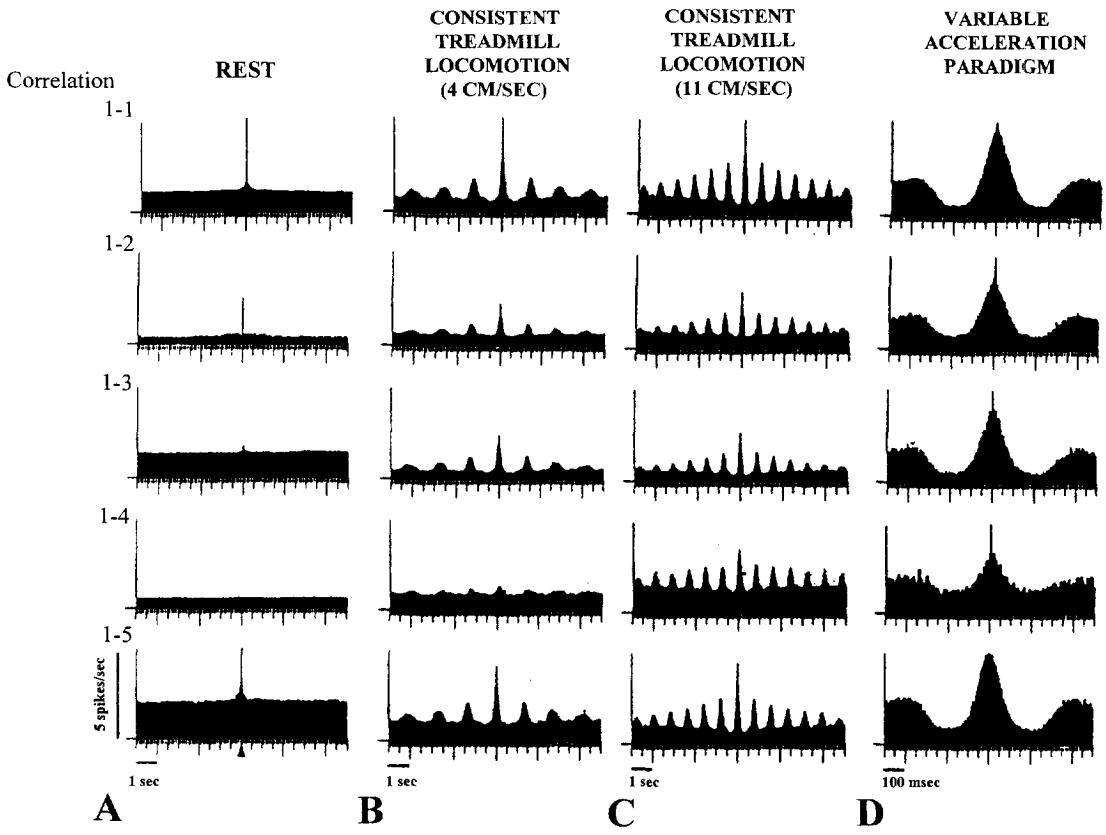

Fig. 5. Olivary oscillations are a function of locomotor behaviour. Cross-correlations of olivary discharge from the same five DAO neurons recorded across several behavioural states (panels A–D) demonstrate rhythmic discharge during treadmill locomotion. In all cases, the uppermost correlograms are autocorrelograms (cell 1); the remainder (cells 2–5) are cross-correlograms, correlating activity with cell 1. During quiet rest (panel A), olivary cells recorded simultaneously did not discharge rhythmically, although synchronized activity was observed. However, correlograms of olivary discharge recorded during consistent speed locomotion (panels B,C) reveal oscillations in phase with the step cycle (0.7–1.5 Hz). The frequency and distribution of peaks in these correlograms (B,C) resemble those averaged around the step cycle (compare with Fig. 6), as well as correlograms of step cycle time-points (Fig. 7). During a more complex treadmill paradigm employing unpredictable changes in treadmill speed (panel D), and thus gait (variable acceleration paradigm), olivary populations conisistently oscillated at a frequency of 3 Hz despite inconsistent gait, which may reflect the minimum inter-step interval. [A different time base is used for consistent speed locomotion (5 s) vs variable speed locomotion (0.5 s), because these time bases best permit visualization of oscillation frequency for the two paradigms. In the second case, IO frequency becomes variable at longer step cycle frequencies; therefore rhythmic discharge dissipates as the time base is lengthened. In contrast to Fig. 4, the highest peak is eliminated in these correlograms in order to better visualize the rhythmic discharge pattern. Due to this modification, the *y*-axis more accurately reflects the firing rate rather than the correlation coefficient] (n=74 neurons, five rats).

of discharge (see 10×10 cross-correlogram matrix, Fig. 4). The average correlation coefficient for this population was 0.23 ± 0.08; peak-to-trough amplitude of the oscillation averaged 4.4 ± 0.6 spikes/s.

Olivary rhythmicity during missed steps

Olivary discharge recorded during consistent speed locomotion revealed that a single "missed step" was accompanied by continued rhythmic olivary discharge at a frequency similar to that observed during regular gait. As presented in the stripchart record (Fig. 8A), a step occurs, on average, every 0.7 s; in all cases olivary discharge occurs before foot-fall (indicated by *). In one instance, a missed step occurs (at arrow); however, an olivary spike occurs at the appropriate timepoint for the ongoing frequency. This stripchart record is representative of five cells which were entrained to the step cycle; these cells, which exhibited upper limb receptive fields, discharged at transitions from swing-to-stance. This phenomenon was seen to occur in 12 different cases (three rats), and suggests that an endogenous olivary rhythm may at least be partly responsible for rhythmic olivary discharge during treadmill locomotion.

Rhythmic olivary discharge was also correlated with "missed steps" during variable speed treadmill locomotion, as demonstrated by the strip chart

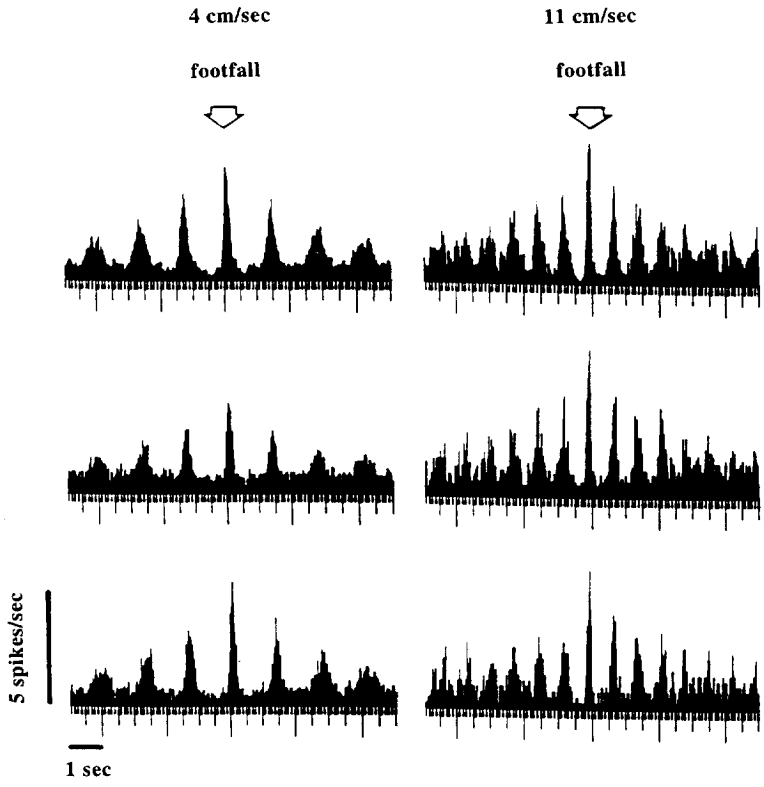

Fig. 6. Patterns of step cycle-correlated discharge during consistent treadmill locomotion. Peri-event histograms of DAO discharge averaged around the time of foot-fall during consistent gait at treadmill speeds of 4 (left) or 11 (right) cm/s reveal rhythmic patterns of discharge similar to correlograms of olivary discharge. (Compare with Figs 5 and 7) (n=74 neurons, five rats).

records in Fig. 8B. Although rhythmic olivary bursts can be correlated in most cases with the times preceding foot-fall, in cases where two steps occur at a different frequency, the rhythmic nature of olivary activity is maintained at a relatively constant frequency (3 Hz); thus olivary "bursts" can be uncoupled from the step cycle when erratic steps occur (n=20 neurons, four rats). This was true for consistent speed locomotion, as well as for step cycle-correlated discharge during a variable acceleration paradigm. Despite the variability in treadmill speed, step cycle activity was relatively regular.

Training effect

Rhythmic olivary discharge during constant speed locomotion (11 cm/s) was a function of the step cycle. At the onset of training, both gait and olivary discharge were initially irregular. After several days of training, however, once consistent gait became established, olivary discharge developed a consistent rhythmicity, in phase with the step cycle (Fig. 9A). By day 3 this rhythmicity was beginning to emerge (a, left panel), and was fully apparent by day 6 of training at 1.3–1.5 Hz (b, right panel). (Average day to attain maximal olivary rhythmicity was 5.2 ± 1.5). Autocorrelograms of the step cycle resemble olivary discharge patterns (data not shown). The variable acceleration paradigm was initiated only after the constant speed locomotion paradigm became routine. In contrast to constant speed locomotion, 3 Hz rhythmic activity was noted as early as day one of the variable acceleration paradigm (Fig. 9Ba, left panel), before training was complete, although rhythmicity became more consistent and reached maximal levels by day three of training (Fig. 9Bb, right panel). (Average day to attain maximal olivary rhythmicity with this paradigm was 3.4 ± 0.5). As noted above, autocorrelograms of the step cycle appear identical to autocorrelograms of olivary discharge throughout the training period (data not shown). Thus, these findings suggest that patterns of olivary activity correlated with constant and variable speed locomotion develop over a different time-course.

Olivary response to electrical stimulation of afferent input

Electrical stimulation of the hindlimb using 2 Hz pulses of 300–1200 μA produced robust responses in 40% of the neurons recorded. A resonant 6 Hz response was noted in 90% of the responsive neurons recorded. (For an example of this pattern of response, see Fig. 10). Stimulation outside of the identified receptive field area (i.e. snout) produced no

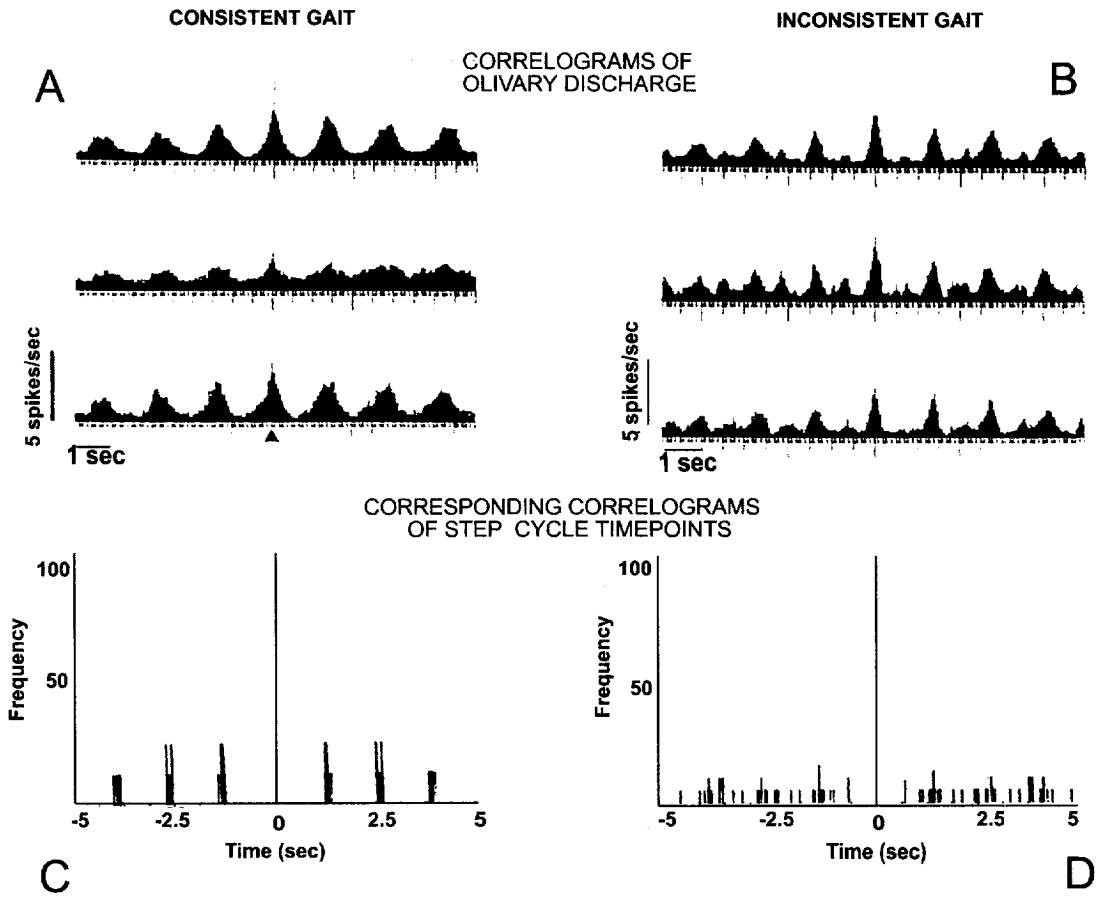

Fig. 7. Olivary neurons discharge rhythmically despite inconsistent gait. Both correlograms of olivary discharge (A,B) and step cycle time-points (C,D) are presented for different gait conditions. Correlograms of olivary discharge constructed during periods of consistent, regular gait (A) and inconsistent gait (B) during treadmill locomotion (at 4 cm/s) reveal rhythmic olivary discharge in both cases. Correlograms of step cycle time-points averaged around foot-fall (C,D) constructed concomitantly with DAO recordings allow comparisons of gait with DAO discharge. Discharge patterns during consistent gait (A) were similar in frequency and distribution to patterns of step cycle time points analysed concomitantly, as demonstrated by the correlogram in C. However, discharge during inconsistent gait (B) was of a similar frequency to that assessed during consistent gait but with a higher harmonic (A), and also of a rhythmic nature compared to an arrhythmic step cycle pattern as revealed by the correlogram of the step cycle (D). These data suggest that rhythmic olivary discharge is entrained to the step cycle, but can maintain an endogenous rhythm during transient (<3 s) periods of inconsistent gait. (n=50 neurons, five rats).

such response (data not shown) (n=20 neurons recorded from three rats). In general, IO discharge was capable of following a stimulation frequency of 12 Hz or less. At stimulation frequencies of 1–4 Hz, IO frequency was 3 × the input stimulation frequency; at stimulation frequencies of 5–6 Hz, an IO frequency was 2 × the input frequency, and at stimulation frequencies of 7–12 Hz, IO frequency equalled input frequency, with lesser harmonics possible at the higher frequency ranges (similar to those shown in Fig. 5B).

DISCUSSION

The results from the present study suggest that the IO exhibits oscillatory patterns of discharge only during rhythmic behavioural and stimulation paradigms relevant for the receptive field studied. Consistent, rhythmic behavioural patterns were accompanied by rhythmic IO discharge patterns of identical frequencies. Rhythmic locomotion produced a 0.7–1.5 Hz oscillation in neurons with receptive fields on the proximal limbs. Locomotion using a variable acceleration paradigm produced variable gait patterns, but was also accompanied by a 3 Hz olivary oscillation. In contrast, olivary discharge obtained during awake states of non-movement did not exhibit rhythmic behaviour. The frequency of the oscillation observed was dependent upon rhythmic movement of the relevant limb. These results suggest that the the oscillatory properties of the IO may be dependent upon both an endogenous capacity to oscillate as well as a response to relevant sensorimotor input.

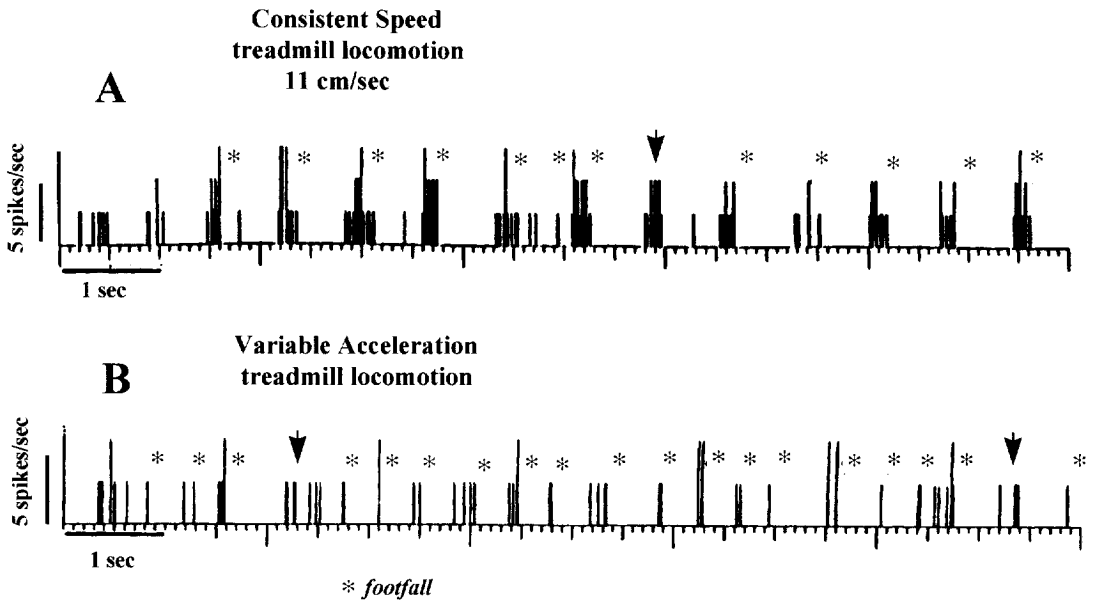

Fig. 8. Rhythmic DAO discharge persists despite "missed" steps. Strip chart, continuous time records of DAO discharge recorded during consistent speed treadmill locomotion (A) at 11 cm/s or during the variable acceleration paradigm (B) reveal "bursts" of olivary discharge which precede foot-fall (*). Although gait is consistent for both paradigms, when a missed step occurs (i.e. out of sequence with the ongoing frequency of stepping-depicted by arrow), an olivary "burst" occurs in phase with the ongoing frequency. For this animal, five cells were entrained to step cycle rhythmicity; these regularly firing cells all discharged at transitions from stance-to-swing. These data suggest that rhythmic olivary discharge may be a function of both inherent rhythmicity and the ongoing rhythmic behaviour. These results are representative of those determined in three rats (12 neurons), A, or four rats (20 neurons), B.

Intrinsic timing function

These data are consistent with the theory that the IO serves as an internal timing device for rapid movements of the limbs. Similar rhythmic patterns of climbing fibre discharge from the IO have been described during whisker movement or tongue protrusions,[30] respectively. Although there have been other reports of IO discharge coupled to the step cycle,[10] this correlation has not always been noted.[1] In the present study, several factors may have permitted observation of rhythmic discharge correlated with rhythmic movement: i) cells with proximal rather than distal limb receptive fields were tested, and ii) ensembles of neurons were analysed, as rhythmic discharge has been reported to be an emergent network property[12,30] rather than a single neuron property.

Intrinsic vs extrinsic sources of inferior olive oscillations

The fact that rhythmic IO discharge was tightly coupled to rhythmic movement supports the concept that the IO drives rhythmic movement through its control of cerebellar activity. However, rhythmic IO discharge observed during constant speed treadmill locomotion could reflect either intrinsic oscillatory membrane properties or response to rhythmic sensorimotor input or both. *In vitro* studies conducted by Llinas and Yarom[16,17] have characterized subthreshold membrane oscillations of the IO. These intrinsic rhythmic changes in membrane potential are dependent upon a low-threshold calcium conductance which de-inactivates at hyperpolarizing membrane potentials and is tetrodotoxin-insensitive. Rhythmic spiking could be achieved with administration of tremor-inducing drugs such as harmaline.[15,17] The ability of olivary neurons to exhibit synchronized oscillations is further dependent upon electrotonic coupling via gap junctions.[9,20,26] Sensory signals to the IO are either amplified or dampened depending upon the phase matching of the membrane potential with the timing of the sensory input with this intrinsic oscillatory pattern.[17] *In vivo*, the rhythmic timing of complex spikes of cerebellar Purkinje cells, which reflects uniformly conducted IO activity,[27] has been shown to correlate with rhythmic movement of the whiskers or tongue[6,14,21,30] and resonates in phase with stimulation of peripheral afferents. Somatosensory input to the IO projects from spinal cord, dorsal column nuclei and somatosensory cortex,[5,18,28,29] suggesting the possibility for complex modulation of IO discharge by ongoing sensorimotor activity. However, one recent study[30] demonstrated rhythmic olivary activity correlated with rhythmic tongue movements in a rat with trigeminal deafferentation, a finding strongly suggestive of an intrinsic rhythmic source.

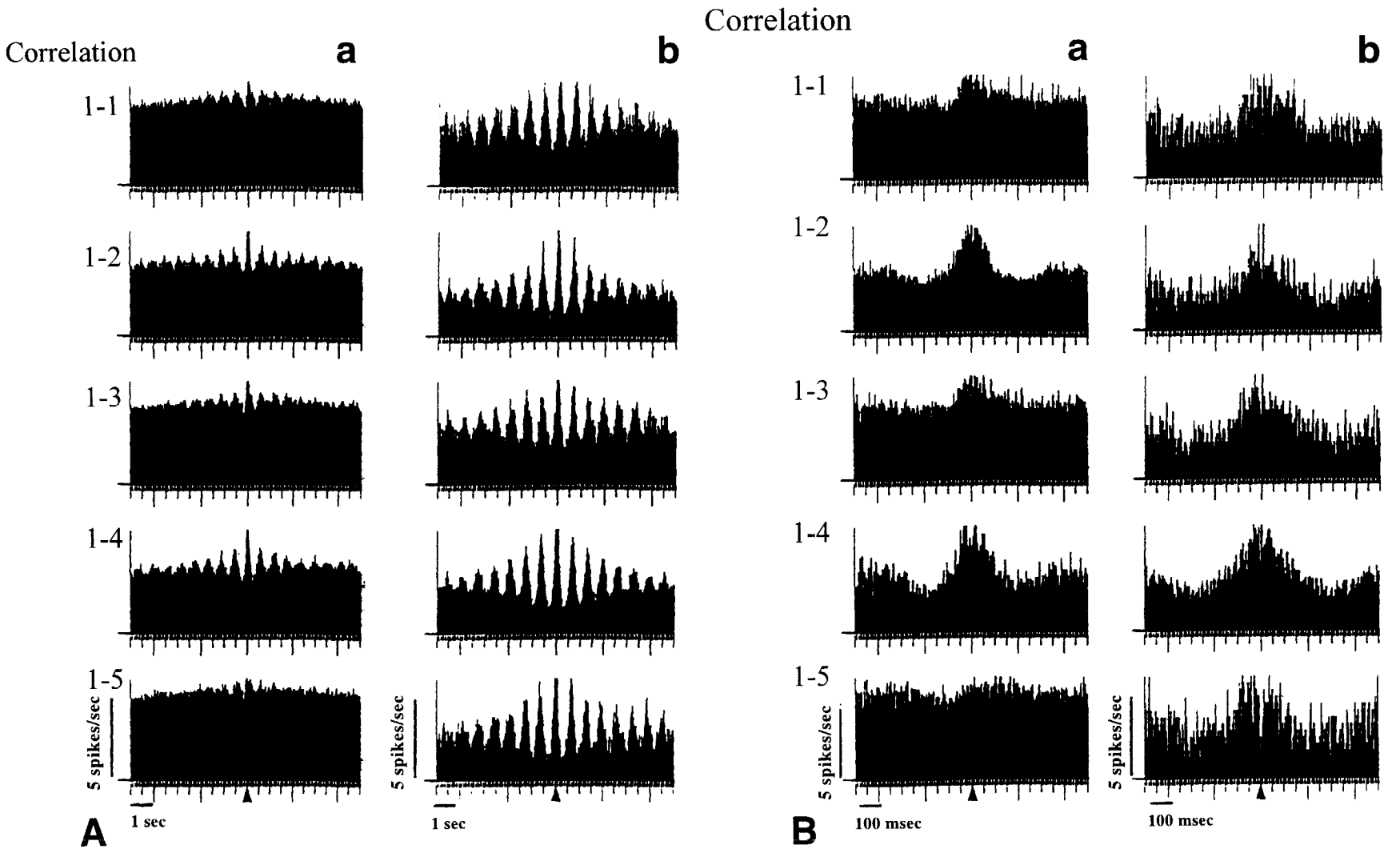

Fig. 9. Development of olivary rhythmicity. Rhythmic olivary discharge develops in association with step cycle rhythmicity during early treadmill training, as revealed by these auto-(top panel), and cross-correlograms (bottom panels, cell no. 1, driver). A) Olivary rhythmicity during consistent speed treadmill locomotion develops to maximal levels by the sixth trial (b, right panel), from minimal levels first observed at the third trial (a, left panel). B) In contrast, the 3 Hz rhythm observed during the variable acceleration paradigm is initially observed during the first trial (a, left panel), and becomes maximal by the third trial (b, right panel). These patterns of discharge resemble step cycle patterns assessed concomitantly (data not shown). (These data are representative of 10 trials assessed in five rats).

Fig. 10. Rhythmic olivary discharge during rhythmic stimulation of the upper forelimb. Strip chart records reveal that stimulation of the right forelimb at a frequency of 2 Hz results in robust responses from the DAO at this frequency (arrow), with harmonics observed at a frequency of 6 Hz. This figure is representative of responses recorded from 20 neurons recorded from three rats.

In the present study the rhythmic timing of the sensorimotor event could be partially uncoupled from the rhythmic discharge pattern of the IO. Periods of inconsistent gait were accompanied by olivary discharge at frequencies with harmonics in phase with the discharge patterns recorded during consistent gait at the same treadmill speed. More compelling evidence, however, comes from the finding that rhythmic olivary discharge was maintained during isolated cases of non-rhythmic gait (i.e. missed steps) during either the constant or variable speed treadmill locomotion paradigms. In this case, the step cycle and discharge pattern were not phase matched. Periods of "missed steps" were accompanied by rhythmic DAO spikes in phase with the ongoing step cycle rhythm. It is important to note that rhythmic IO discharge was maintained only during short interruptions of consistent gait; this suggests an intrinsic source for the oscillation. However, longer intervals of interrupted gait (i.e. more than 3 s) could reset the IO rhythm to the ambient step cycle frequency. In fact, periods of quiet rest were unaccompanied by rhythmic IO discharge. Thus, taken together these data suggest that both intrinsic oscillatory properties and sensorimotor input may influence discharge properties of inferior olivary neurons. These data are also completely consistent with a role for the IO as a timer of rhythmic movement whose function is to drive the movement. These conclusions are similar to those reported[30] for complex spike discharge correlated with rhythmic tongue movement.

Variable acceleration treadmill paradigm

In addition, the variable speed paradigm produced a variable gait which, however, exhibited a minimum inter-peak interval, reflected by a maximum speed of 3 Hz. This was consistent despite the random occurrence of longer inter-peak intervals. Analysis of synchronized neuronal populations revealed one pacemaker for this 3 Hz rhythm, with however, a number of fragmented synchronized neuronal pools. The meaning of this phenomenon is not clear, but may reflect multiple pacemakers for a variable speed paradigm.

Electrical stimulation

Electrical stimulation of peripheral afferents produced responses at resonant frequencies in phase with the stimulation. This finding is consistent with the reports from other labs demonstrating similar resonating responses of climbing fibres to stimulation of peripheral afferents.[6,14,21] Collectively, these data suggest that sensory input, delivered as a single pulse or at frequencies in phase with olivary discharge, has the capacity to reset the frequency of olivary oscillations.

Oscillation frequency and the step cycle

The maximal oscillation frequency of 3 Hz obtained from cells with receptive fields on the limbs may be related to maximal rates of stepping. A maximal step cycle frequency of 3 Hz even at higher treadmill speeds is due to a change from trot to gallop, a gait which involves fewer steps but an increase in stride length. Higher oscillation frequencies have been obtained from climbing fibres projecting from olivary neurons with whisker or tongue receptive field properties;[14,21,30] in contrast to limb movement, maximal movement of the whisker and tongue is in the 8–10 Hz range. Intrinsic channel properties may also contribute to the slower oscillation frequency observed in the present study. *In vitro* studies have revealed that under depolarizing conditions, olivary neurons exhibit subthreshold membrane oscillation of 3–5 Hz; only under hyperpolarizing conditions were 8–10 Hz oscillations of membrane potential observed.[11,13] In the present study, oscillating discharge was only observed during limb movement. Rhythmic discharge was not observed during awake non-movement conditions. Thus, sensorimotor input was required for these neurons to exhibit oscillatory patterns of discharge.

Development of rhythmic discharge

Development of rhythmic olivary discharge paralleled development of consistent gait frequencies as the animal became accustomed to treadmill

locomotion. Rhythmic olivary discharge correlated with gait developed over a five to six day period during constant speed locomotion. However, the 3 Hz olivary rhythmicity observed during the variable acceleration paradigm was apparent on day one. The faster development of rhythmic olivary discharge patterns during this paradigm may be due to the fact that i) the animal was already trained to run on the treadmill and ii) the 3 Hz rhythm reflects the minimum inter-step interval, which may be a more intrinsic gait property than consistent gait.

CONCLUSION

In conclusion, these data demonstrate that in the awake locomoting rat, discharge from the IO exhibits rhythmic discharge only during rhythmic locomotor and stimulation paradigms, as has been reported for tongue and lip movement.[21,30] The data further suggest that the rhythmic nature of IO discharge may be a result of both intrinsic properties as well as a result of sensorimotor input, which may serve to drive or reset endogenous rhythmicity. Synchronized oscillating IO discharge has been described as an internal timing mechanism which drives rhythmic movement.[12] The 3 Hz olivary oscillations observed in the present study during variable gait may subserve such a timing function.

Acknowledgements—The author is grateful to J. K. Chapin for developing the neuronal ensemble recording technology. This work was supported by USAF F4962093-1-0136.

REFERENCES

1. Armstrong D. M., Edgley S. A. and Lidierth M. (1988) Complex spikes in Purkinje cells of the paravermal part of the anterior lobe of the cat cerebellum during locomotion. *J. Physiol.* **400,** 405–414.
2. Azizi S. A. and Woodward D. J. (1987) Inferior olivary nuclear complex of the rat: morphology and comments on the principles of organization within the olivocerebellar system. *J. comp. Neurol.* **263,** 467–484.
3. Barmack N. H., Fagerson M., Fredette B. J., Mugnaini E. and Shojaku H. (1993) Activity of neurons in the beta nucleus of the inferior olive of the rabbit evoked by natural vestivular stimulation. *Expl Brain Res.* **94,** 203–215.
4. Benardo L. S. and Foster R. E. (1986) Oscillatory behavior in inferior olive neurons: mechanism, modulation, cell aggregates. *Brain Res. Bull.* **17,** 773–784.
5. Berkley K. J. and Hand P. J. (1978) Projections to the inferior olive of the cat. II. Comparisons of input from the gracile, cuneate and the spinal trigeminal nuclei. *J. comp. Neurol.* **180,** 253–264.
6. Bloedel J. R. and Ebner T. J. (1984) Rhythmic discharge of climbing fibre afferents in response to natural peripheral stimuli in the cat. *J. Physiol.* **352,** 129–146.
7. Chapin J. K. and Nicolelis M. A. L. (1996) Neural network mechanisms of oscillatory brain states: characterization using simultaneous multi-single neuron recordings. *Electroenceph. clin. Neurophysiol.* (in press).
8. Gellman R., Gibson A. R. and Houk J. C. (1985) Inferior olivary neurons in the awake cat: detection of contact and passive body displacement. *J. Neurophysiol.* **54,** 40–60.
9. Gwyn D. G., Nicholson G. P. and Flumerfelt B. A. (1978) The inferior olivary nucleus of the rat: a light and electron microscopic study. *J. comp. Neurol.* **174,** 489–520.
10. Kim J. H., Wang J. J. and Ebner T. J. (1987) Climbing fiber afferent modulation during treadmill locomotion in the cat. *J. Neurophysiol.* **57,** 787–802.
11. Lampl I. and Yarom Y. (1993) Subthreshold oscillations of the membrane potential: a functional synchronizing and timing device. *J. Neurophysiol.* **70,** 2181–2186.
12. Llinas R. R. (1991) The noncontinuous nature of movement execution. In *Motor Control: Concepts and Issues* (eds Humphrey D. R. and Freund H.-J.), pp. 223–242. Wiley, New York.
13. Llinas R., Baker R. and Sotelo C. (1974) Electrotonic coupling between neurons in the inferior olive. *J. Neurophysiol.* **37,** 560–571.
14. Llinas R. and Sasaki K. (1989) The functional organization of the olivo-cerebellar system as examined by multiple Purkinje cell recordings. *Eur. J. Neurosci.* **1,** 587–602.
15. Llinas R. and Volkind R. A. (1973) The olivo-cerebellar system: functional properties as revealed by harmaline-induced tremor. *Expl Brain Res.* **18,** 69–87.
16. Llinas R. and Yarom Y. (1981) Electrophysiology of mammalian inferior olivary neurones *in vitro*. Different types of voltage-dependent ionic conductances. *J. Physiol.* **376,** 163–182.
17. Llinas R. and Yarom Y. (1986) Oscillatory properties of guinea-pig inferior olivary neurones and their pharmacological modulation: an *in vitro* study. *J. Physiol.* **376,** 163–182.
18. Molinari H. H., Dostrovsky J. O. and El-Yassir N. (1990) Functional properties of dorsal horn neurons that project to the dorsal accessory olive. *J. Neurosci.* **64,** 1704–1711.
19. Nicolelis M. A. L., Baccala L. A., Lin C.-S. and Chapin J. K. (1995) Synchronous neuronal ensemble activity at multiple levels of the somatosensory system during tactile exploratory movements. *Science* **268,** 1353–1358.
20. Ruigrok T. J. H., DeZeeuw C. I., Vender Burg J. and Voogd J. (1990) Intracellular labeling of neurons in the medial accessory olive of the cat: I. Physiology and light microscopy. *J. comp. Neurol.* **300,** 462–477.
21. Sasaki K., Bower J. M. and Llinas R. (1989) Multiple Purkinje cell recordings in rodent cerebellar cortex. *Eur. J. Neurosci.* **1,** 572–586.
22. Sears T. A. and Stagg D. (1976) Short-term synchronization of intercostal motoneurone activity. *J. Physiol., Lond.* **263,** 357–381.
23. Smith S. S. (1995) Sensorimotor-correlated discharge recorded from ensembles of cerebellar Purkinje cells varies across the estrous cycle. *J. Neurophysiol.* **74,** 1095–1108.
24. Smith S. S. and Chapin J. K. (1996) Estrous hormones and the olivo-cerebellar circuit I: Contrast enhancement of sensorimotor-correlated Purkinje cell discharge. *Expl Brain Res.* **1113,** 371–384.
25. Smith S. S. and Chapin J. K. (1996) Estrous hormones and the olivo-cerebellar circuit II: Enhanced selective sensory gating processes as putative error signalling mechanisms. *Expl Brain Res.* **1113,** 385–392.

26. Sotelo C., Llinas R. and Baker R. (1974) Structural study of inferior olivary nucleus of the cat: morphological correlates of electrotonic coupling. *J. Neurophysiol.* **34,** 541–559.
27. Sugihara I., Lang E. J. and Llinas R. (1993) Uniform olivocerebellar conduction time underlies Purkinje cell complex spike synchronicity in the rat cerebellum. *J. Physiol.* **470,** 243–271.
28. Swenson R. S. and Castro A. J. (1983) The afferent connections of the inferior olivary complex in rats. An anterograde study using autoradiographic and axonal degeneration techniques. *Neuroscience* **8,** 259–275.
29. Swenson R. S., Sievert C. F., Terreberry R. R., Neafsey E. J. and Castro A. J. (1989) Organization of cerebral cortico-olivary projections in the rat. *Neurosci. Res.* **7,** 43–54.
30. Welsh J. P., Lang E. J., Sugihara I. and Llinas R. (1995) Dynamic organization of motor control within the olivocerebellar system. *Nature* **374,** 453–457.
31. Wiegner A. W. and Wierzbicka M. M. (1987) A method for assesing significance of peaks in cross-correlation histograms. *J. Neurosci. Meth.* **22,** 125–131.
32. Yarom Y. and Llinas R. (1987) Long-term modifiability of anomalous and delayed rectification in guinea pig inferior olivary neurons. *J. Neurosci.* **7,** 1166–1177.

(*Accepted* 14 *April* 1997)